Full-aperture interferometric test of convex secondary mirrors using holographic test plates

J. H. Burge and D. S. Anderson

Steward Observatory Mirror Lab, University of Arizona
Tucson, Arizona 85721

ABSTRACT

Convex secondary mirrors are notoriously difficult to fabricate because of the tremendous cost and difficulty of making accurate measurements of the optical surfaces. The new 6.5- and 8-m-class telescopes require secondary mirrors that are larger, more aspheric, and more accurately figured than those for existing telescopes. The challenge of measuring these giant optics has spurred the development of a new measurement technique using holographic test plates. This test uses a full-aperture test plate with a computer-generated hologram (CGH) fabricated onto the spherical reference surface. When supported a few millimeters from the secondary and properly illuminated with laser light, an interference pattern is formed that shows the secondary surface errors. The hologram consists of annular rings of metal drawn onto the curved test plate surface using a custom-built writing machine. The accuracy of the surface measurement using this technique is expected to be 35 nm P-V and 6 nm rms for a 1.7-m secondary mirror for the MMT. Considerably higher accuracy is expected for less aspheric surfaces.

1. INTRODUCTION

A new interferometric test has been developed to allow efficient testing of highly aspheric secondary mirrors to the accuracy required by the next generation optical telescopes. This test is a hybrid of two commonly used optical measurement techniques, Fizeau test plate interferometry and the use of computer-generated holograms. The aspheric secondary mirrors are measured using spherical test plates with computer-generated holograms. The holograms, consisting of annular rings of chrome, are written onto the spherical reference surface. The positions of the rings are chosen to give the desired shape of the diffracted wavefront, and the width of the rings is controlled to give high fringe visibility. The test is performed by supporting the holographic test plate a few millimeters from the secondary mirror and illuminating with laser light (see Fig. 1). The interference pattern is viewed through the test plate and imaged onto a CCD camera for analysis. By pushing the secondary mirror or the test plate, phase shifting interferometry is used to obtain high resolution data. This paper gives an overview of the CGH test, a summary of results a prototype test, and a discussion of plans for implementing this test for large secondary mirrors at the Steward Observatory Mirror Lab. The successful measurement of a small secondary mirror to high accuracy using a prototype test plate is described in a separate paper in these proceedings.[1]

The benefits of this test over existing methods of measuring convex secondary mirrors are its inherent accuracy, the efficiency, and the overall cost. As a Fizeau test, this is a differential measurement between a reference surface and the optic being tested. This minimizes errors due to illumination, vibration, and seeing. Unlike the Hindle shell test or the use of a null lens looking through the back surface, the refractive index inhomogeneity of the large optics does not affect the test. The accuracy of the test is limited only by the quality of a concave spherical surface and the accuracy of the ring locations. Both can be made and verified to high accuracy. Since

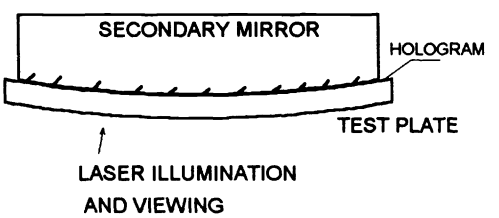

Figure 1. Layout of holographic test of a secondary mirror. The test plate has a concave reference spherical surface with a ring pattern drawn onto it.

0-8194-1494-8/94/$6.00

the test is not affected by vibration and seeing, it is quickly performed without struggling to control the environment. The alignment of the test is easily accomplished by moving the test plate to null the fringe pattern. A measurement of the full aperture, with hundreds of points across the diameter, can be made to nanometer precision in only minutes. A large part of the cost of the holographic test is the development of the large writer and an optical system for illuminating the test and viewing the fringes. The costs of both of these will be shared over several telescope projects.

We plan to implement this test for the efficient fabrication of highly aspheric secondary mirrors at the Steward Observatory Mirror Lab. Table 1 lists several of the proposed secondary mirrors to be measured with CGH test plates. We are currently developing the equipment required to perform these measurements, as well as the facility for handling, grinding, and polishing these large optics.

Table 1. Proposed convex secondary mirrors to be measured using CGH test plates.

	MMT	ARC F/8	Sloan	MMT *f*/9	MMT *f*/15	MMT *f*/5	LBT *f*/4
diameter (mm)	260	838	1143	996	620	1653	1170
radius of curvature R (mm)	1484	3167	7194	2806	1663	5022	3294
conic constant K	-1.430	-2.185	-12.110	-1.749	-1.397	-2.640	-3.236
surface sagitta (mm)	5.7	27.7	22.7	44.2	28.9	68.0	51.9
P-V asphere (microns)	3.9	66.3	108.4	152.2	87.7	304.0	331.4
focal ratio	2.85	1.89	3.15	1.41	1.34	1.52	1.41

2. DESCRIPTION OF TEST

Convex spherical surfaces are commonly measured with matching concave test plates. When the test plate is supported near the convex optic and illuminated with sufficiently coherent light, fringes of interference show the shape difference between the two parts. The concave spherical test plate is verified independently from its center of curvature. Similarly, convex non-spherical surfaces may be tested using concave test plates that have the matching aspheric shape. This adds cost and complexity by requiring the fabrication and measurement of the additional concave aspheric surface. The holographic test effectively uses diffraction from the hologram to make the test plate work as if it had the appropriate aspheric shape.

2.1 DEFINITION OF REFERENCE AND TEST WAVEFRONTS

The holographic test uses the interference between a reference and a test wavefront to determine the shape of the convex optic. Light diffracted from the hologram on the spherical surface forms the reference wavefront and light reflected from the secondary forms a test wavefront (see Fig. 2). The test plate is illuminated with light that is transmitted to strike the secondary mirror at normal incidence for all points on the mirror. This light reflects back onto itself to form the test wavefront. The reference wavefront is formed by diffraction from the ring pattern on the reference sphere. The CGH is designed to diffract this reference beam to match an ideal test wavefront, so this beam also retraces the incident path. (This is known as a Littrow configuration for a grating.) To perform a measurement, laser light from a point source is used so the reflected wavefronts converge to a conjugate image point, where an aperture blocks undesired orders of diffraction.

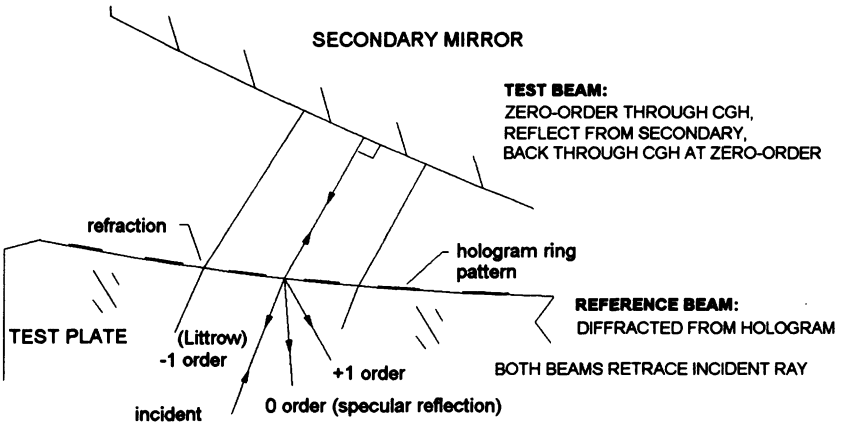

Figure 2. Definition of reference and test wavefronts. A reference beam diffracted from the hologram interferes with the test beam reflected from the secondary.

The test beam and the reference beam coincide everywhere in the system except in the gap between the secondary and the test plate. Both beams pick up wavefront errors ΔW_{system} from illumination optics and refractive index variations in the test plate. Irregularities in the test wavefront ΔW_{test} are also caused by the reference surface and secondary mirror figures, leading to

$$\Delta W_{test} = \Delta W_{system} + 2(1-n)\Delta S_{ref} + 2\Delta S_{test} \tag{1}$$

where ΔS_{ref} is the surface error in the test plate (+ for bumps as viewed from concave side),
n is the refractive index of the test plate, and
ΔS_{test} is the surface error in the optic being tested.

Likewise, the irregularity in the reference wavefront ΔW_{ref} is shown to be

$$\Delta W_{ref} = \Delta W_{system} - 2n\Delta S_{ref} + \Delta W_{CGH}, \tag{2}$$

where ΔW_{CGH} is the wavefront error due to errors in the CGH.

Phase shifting interferometry measures the difference in these two wavefronts [ΔW_{test} - ΔW_{ref}] to several nanometers. The irregularity in the shape of the secondary mirror is then

$$\Delta S_{test} = \frac{1}{2}\left[\Delta W_{test} - \Delta W_{ref}\right] + \Delta S_{ref} - \frac{1}{2}\Delta W_{CGH}. \tag{3}$$

Clearly the figure errors in the test plate and the hologram errors must be kept small. However, known errors in the surface or hologram can be backed out of the secondary test as long as these errors can be measured and mapped accurately. The spherical reference surface can be independently measured from its center of curvature. Azimuthal errors in the test can be determined by rotating the secondary with respect to the test plate. Errors that stay fixed with the test plate are removed from the secondary measurement. The rotationally symmetric component of the hologram can be verified by confirming the ring positions.

2.2 OPTICAL TESTING USING COMPUTER-GENERATED HOLOGRAMS

Optical testing of aspheric surfaces using computer-generated holograms has been used for many years.[2,3] A hologram is generally used to modulate the phase or amplitude of a wavefront, causing it to propagate to form a desired phase front or intensity distribution. A photographically produced hologram may be used to store and play back an existing wavefront.[4] Synthetic holograms may also be specified by a computer and written with an electronic plotter.[5] Computer-generated holograms fall into three classes -- Fourier, Fresnel, and image holograms,[6] depending on the propagation from the CGH. The image hologram, used for optical testing, is the simplest type because the pattern shape is directly computed from desired phase change. The ruling pattern corresponds to a binary representation of the interferogram that would be created at the CGH plane if the incident beam were interfered with the desired beam. These binary rulings cause multiple orders of diffraction that must be filtered out of the final interferogram. These multiple orders are separated at the Fourier transform plane, where a correctly positioned aperture passes only the desired order.

The computer-generated hologram of the image- or interferogram-type may be thought of as locally acting as a diffraction grating. The light diffracted from this ruling splits into distinct orders given by the grating equation,

$$OPD = s(\sin\theta_0 + \sin\theta_m) = m\lambda \tag{4}$$

where the geometry is shown in Fig. 3 and the terms are defined as

OPD = optical path difference for light through adjacent slits
θ_0, θ_m = incident and diffracted angle
m = order of diffraction
s = local ruling spacing.

The CGH is a diffraction grating that uses a spatial variation in ruling frequency to create a desired change in wavefront. The CGH may be interpreted as causing a change in ray directions according to the grating equation (4), or equivalently as directly changing the wavefront phase. When used in m^{th} order, the CGH adds m waves of optical path to the wavefront for each ruling cycle. Also, testing with a CGH may be thought of in terms of a moiré effect. The CGH is a binary representation of the expected fringe pattern formed by interference between the reference and test wavefronts. When the live interference pattern is superimposed on the CGH, a moiré, or spatial frequency "beating" effect is observed. When properly filtered in the frequency domain, these moiré fringes directly give the shape difference between the two wavefronts, thus the shape error in the asphere.

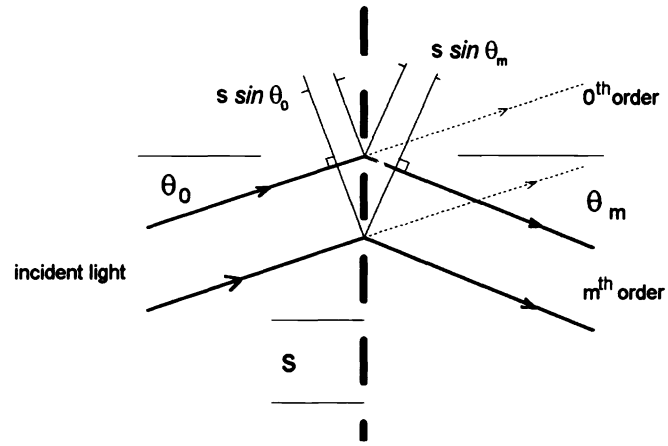

Figure 3. Cross-section of a transmissive diffraction ruling.

Optical testing with a CGH is commonly performed using a configuration similar to that shown in Fig. 4.[7,8] The spatial filter is required to block the unwanted orders of diffraction. A large amount of tilt must be created by the CGH to cause the orders to fan out at the spatial filter, enabling the isolation of a pure reference and pure test beam. This wavefront tilt, equivalent to a carrier frequency in the ruling, must be at least three times greater than the maximum slope of the aspheric wavefront to assure complete separation of orders.[9]

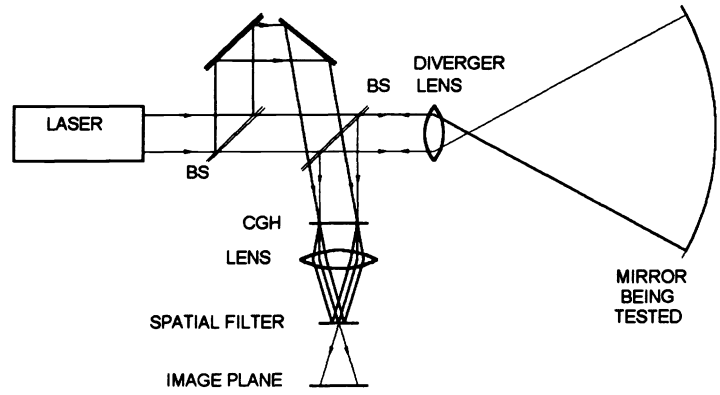

Figure 4. Modified Twyman-Green interferometer for testing an aspheric mirror with a CGH.

Since the CGH is nothing more than a ruling pattern, its errors take the form of spatial distortion in that pattern. The magnitude of the wavefront error due to the distortion is given as the scalar product of the wavefront gradient and the vector distortion,[10] leading to

$$\Delta W(x,y) = -m\lambda \frac{\varepsilon_s(x,y)}{s(x,y)} \tag{5}$$

where $\varepsilon_s(x,y)$ = CGH position error in direction perpendicular to ruled fringes
$s(x,y)$ = local center-to-center ruled fringe spacing
$\Delta W(x,y)$ = wavefront phase error due to pattern distortion at position (x,y) on CGH.

2.3 CIRCULAR COMPUTER-GENERATED HOLOGRAMS

Rather than using a tilt carrier to fan out the orders of diffraction laterally, the rotational CGH preserves the rotational symmetry and disperses the orders along the axis, bringing them to focus at different axial positions. The use of circular holograms for optical testing has been demonstrated by several groups,[11,12] and comparisons between testing with circular and tilt carrier holograms are published.[13,14] Circular CGH's have also been used for certifying the null correctors that measure primary mirrors.[15] There are several advantages to using rotational holograms for testing axisymmetric optics. By preserving the axial symmetry, the hologram design, analysis, and fabrication is reduced from two dimensions to one. The symmetry allows direct certification of the hologram by measuring ring diameters. For testing optics with annular apertures, the inability to test the central region due to leakage of stray diffracted orders is inconsequential.

The spurious orders are blocked using a stop, as shown in Fig. 5. The stop is placed where the light from the desired order comes to focus. The unwanted orders are out of focus and aberrated so only the central region makes it through the aperture. Since an annular pupil is used, an out-of-focus stray order will cause an annular image at the aperture plane. As long as the aperture is smaller than the inner diameter of this annulus, the light from this stray order is completely blocked. The size of the stop is optimized to reject the stray orders while allowing errors in the illumination system.

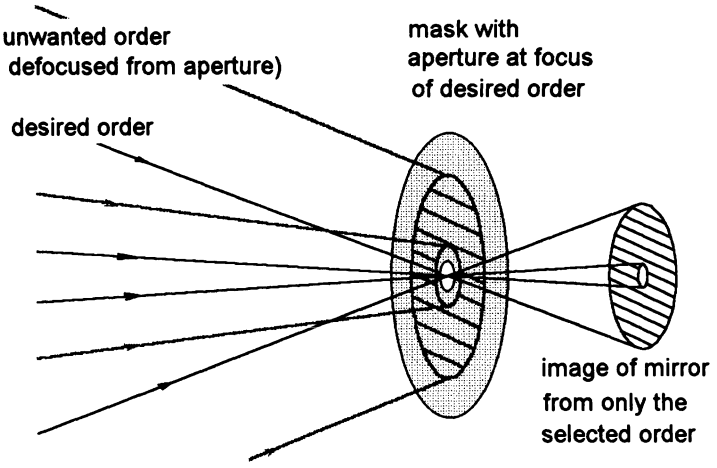

Figure 5. Rejection of stray diffraction orders. The order rejection relies on two principles: (1) the desired order comes to a sharp focus where all other orders are out of focus, and (2) an annular pupil is used. There is a central untested region that is blocked elsewhere.

The order separation requires a trade-off in the design of the test. Large errors in the illumination optics can be tolerated if a large amount of power is built into the CGH, which causes the orders to be widely separated. However, more power in the CGH requires more rings with tighter spacing, which makes the hologram more difficult to fabricate. A compromise between these two effects led to hologram designs allowing slope errors in the system of up to 2 mrad without causing any order leakage.

Even for a perfect illumination system, the aperture may not be made arbitrarily small because the stop acts as a low-pass spatial filter on the surface measurement. The spatial frequency cutoff of the filter, ξ_c, is derived using Fourier optics[16] as

$$\xi_c = \frac{\theta_f}{2\lambda} \tag{6}$$

where ξ_c = spatial frequency of cutoff (cycles per meter at mirror)
θ_f = full angular size of aperture, as viewed from the secondary (radians)
λ = wavelength of light (m).

So a 2 mrad wide aperture gives 3000 cycle-per-meter resolution. Several other high-order diffraction effects were examined and shown to be negligible. The CGH's are designed based on scalar diffraction theory, which is known to be approximate. Rigorous analysis has shown that the diffraction efficiency predicted by this approximation is accurate for rulings with spacings larger than several wavelengths,[17] and the angle of the diffracted light predicted by the scalar theory is exact.[18]

3. TEST DESIGN

The design of the holographic test is divided into the hologram design and the illumination optical system design. The hologram designs involve calculating the ring positions to give the desired phase of the reference wavefront and fixing the width of the rings to match the amplitudes of the test and reference beams. The illumination system is designed to bring the rays of light into the test at the correct angle, to separate diffraction orders, and to minimize the mapping distortion in the test.

3.1 HOLOGRAM DESIGN

The design of a hologram consists of choosing several parameters. For the University of Arizona holograms, the metal that will form the rings was chosen to be chrome and the gap between the test plate and the aspheric mirror was set at 5 mm. The only remaining degree of freedom for a particular secondary mirror is the amount of power or focus in the hologram. The power is chosen to make the wavefront slope large enough that the adjacent orders of diffraction are sufficiently separated that the desired order can be isolated in the presence of illumination errors. Once the CGH power is determined, the required ring pattern and the radius of curvature of the reference surface are fully defined.

Plots of the wavefront slope and shape are shown in Figs. 6 and 7 for the CGH test of the secondary mirror for the Sloan Digital Sky Survey Telescope. The different curves correspond to different amounts of power in the holograms. The amount of power is determined by specifying the radial zone that has the same slope as that at the edge. This zone is indicated by the numbers shown to the right of the curves. The angular separation of the 0 and -2 orders from the -1 order of the reference beam matches the wavefront slope shown in Fig. 6. So if the edge zone is chosen to match the 0.3 radial zone, the power in the hologram will separate the orders by at least 2.75 mrad in the region outside the 0.3 radial zone. The maximum slope for this case is 4.45 mrad at the 0.68 zone. The optical path difference (OPD) function in Fig. 7 matches the hologram design; the ring patterns are defined so there is exactly one ring per wave of OPD.

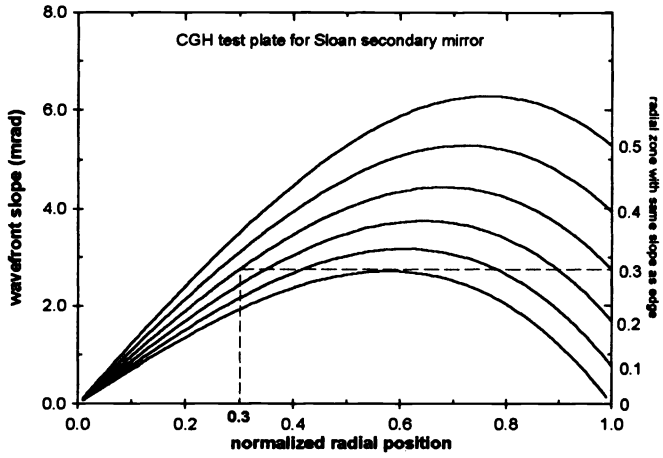

Figure 6. Variation of diffracted wavefront slope with radial position for different amounts of focus. The numbers on the right give the radial zone that has the same slope as the edge.

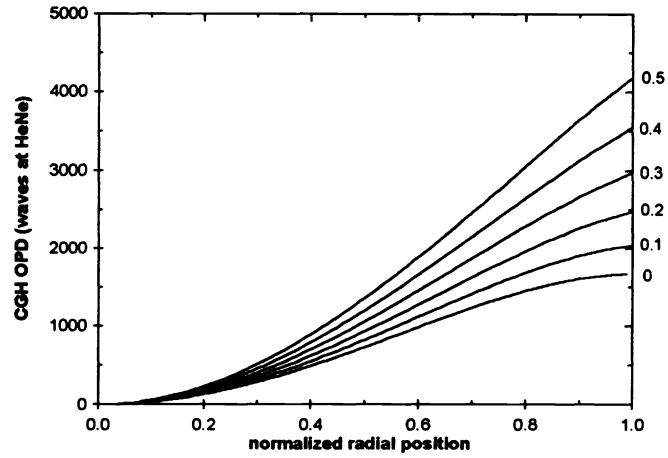

Figure 7. Variation of optical path function defined by hologram with radial position for the different amounts of focus shown in Fig. 6.

The ring spacing corresponding to the above plots are given in Fig. 8. By choosing a convenient amount of power in the hologram for order separation, the spacing remains fairly constant over most of the hologram. It does blow up near the center where the slopes become small, making the central region difficult to test. The effect of a 5 μm radial error in ring center position is computed and shown in Fig. 9 as a function of radial position on the optic. This plot shows how increasing the CGH power increases the sensitivity to hologram errors. If power is chosen so the slope at the 0.3 zone matches the edge slope, 5 μm P-V writing errors will cause the surface measurement to be inaccurate by 11 nm P-V. If the power is increased to where the 0.5 zone is chosen to match the edge slope, the test will be accurate to 16 nm P-V and require 1200 more rings.

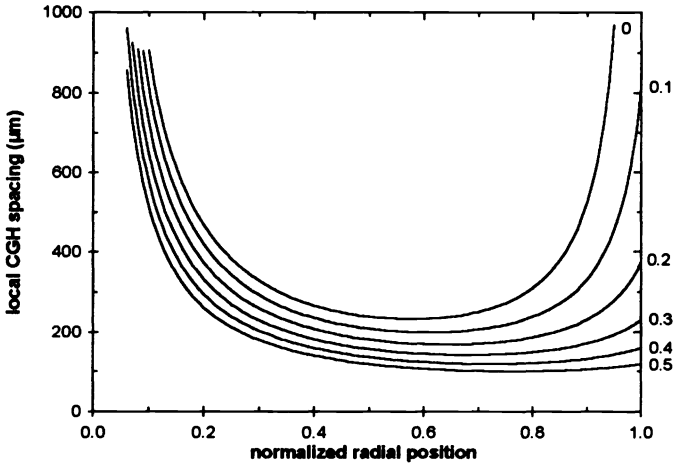

Figure 8. Center to center ring spacing as function of radial position for the different amounts of focus shown in Fig. 6.

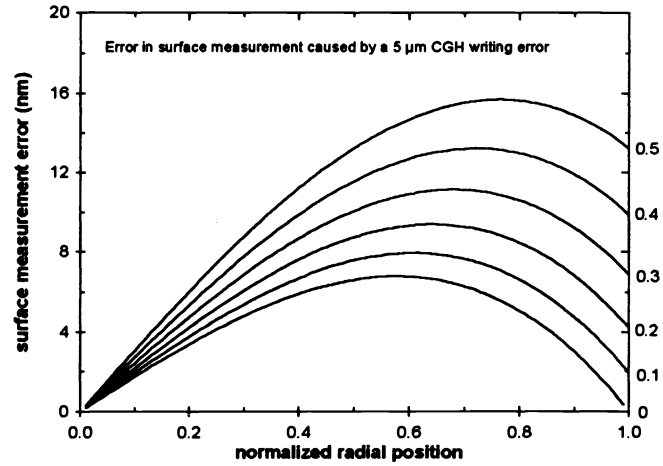

Figure 9. This plot shows the effect of a 5 μm local hologram error on the surface measurement for the different amounts of focus shown in Fig. 6.

The width of the rings is picked to match the intensities of the test and reference wavefronts, giving a high contrast interference pattern. Both reference and test beams are modulated by the hologram, and the far-field distribution is found by taking a Fourier transform. The phase of the reference and test wavefronts are shown to be independent of the line width.

The reference beam is the -1 reflected diffraction order caused by the amplitude and phase modulation from the chrome ruling. The glass-chrome interface reflects 53% of the light with a 156° phase shift. The glass-air interface (the gaps between the chrome) reflects with 4% intensity and 0° phase shift. The fact that light reflects from the glass-air interface with 0° phase shift, while it reflects from the glass-metal interface with nearly 180° phase shift allows the ruling to use this phase modulation and cause the zero order to nearly disappear (See Fig. 10).

The test beam is the zero order transmitted wavefront, which is modulated purely in amplitude by the ruling; the chrome bands project as shadows onto the secondary mirror. Wider bands decrease the 0-order test beam amplitude but increase the -1 order efficiency of the reference beam. For testing bare glass optics using chrome rulings, the optimum width is found for duty cycle D = 18%, as shown in Figs. 10 and 11. The duty cycle D is defined as the ratio of the metal ring width to the center-to-center band separation.

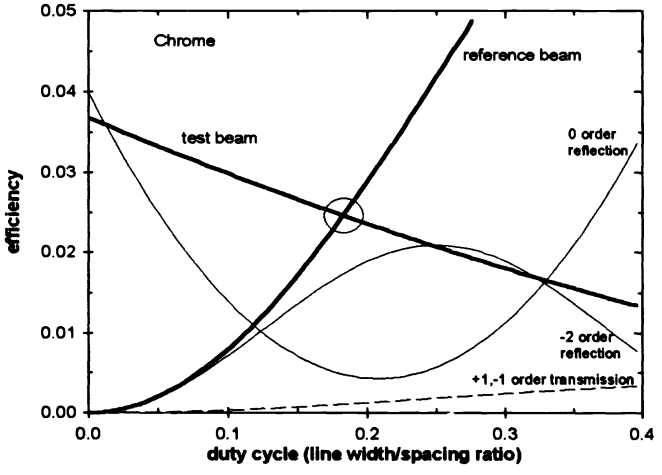

Figure 10. Diffraction efficiency dependence on duty cycle giving the relative intensities of the diffracted orders from chrome rulings.

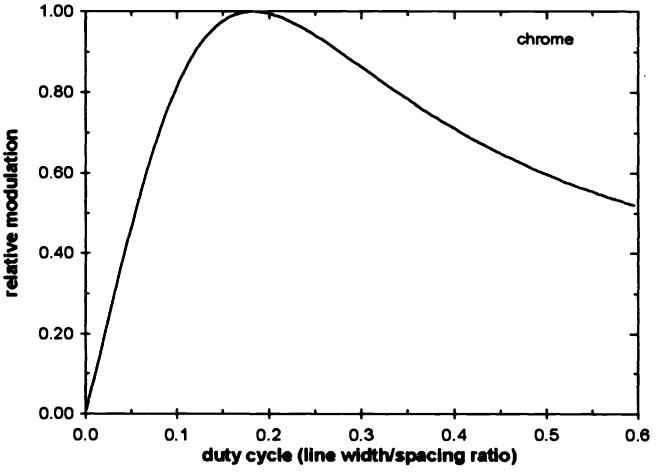

Figure 11. Fringe modulation dependence on duty cycle for a chrome ruling.

After choosing the hologram power that gives the desired order separation, a computer simulation is made of the corresponding concave spherical reference spaced appropriately from the aspheric secondary. The ring pattern is defined by tracing rays normal to the secondary and finding the ray intersections with the spherical test plate surface. The variation in the length of these rays gives the optical path difference *OPD* that the CGH must induce,

$$OPD(r) = l(r) - l(r = 0) \tag{7}$$

where $l(r)$ = gap between reference sphere and secondary on direction defined by secondary normal, and
r = radial position at secondary.

The ring patterns are drawn according to

$$i^{th} \text{ ring defined where } OPD(r) \begin{cases} > OPD(r_0) + i\lambda - \dfrac{D}{2}\lambda \\ < OPD(r_0) + i\lambda + \dfrac{D}{2}\lambda \end{cases} \tag{8}$$

where r_0 = radial position of inside (zeroth) ring.

3.2 DESIGN OF ILLUMINATION SYSTEM

As stated above, the illumination system must get the light pointing in the right direction and must provide a distortion-free image of the secondary to the camera plane. The design of this optical system is straightforward using an optical design computer program. A diverging wavefront is simulated that matches the convex shape of the secondary mirror. The design of the illumination system must bring this wavefront to focus at the order-blocking aperture. At the same time, it must provide linear mapping between the final image and the secondary mirror. The required quality of this system is determined by the smallest angular separation of the spurious orders defined above. Since the illumination system must compensate the large asphericity of the secondary mirror, it is desirable to use aspheric surfaces. The quality of these surfaces need not be high since the test is insensitive to errors below a few arc minutes. Both refractive and reflective illumination systems have been designed and are described below.

The alignment requirements for the illumination system are also relaxed. The system must bring the light to focus at the aperture with slope errors less than the angular order separation, which is about two milliradians. It is important to maintain the autostigmatism of the test, which is accomplished by forcing the reflected light to come to focus *at* the source point. The alignment of the secondary to the test plate is guided by the fringe pattern. The mirror is tilted and translated axially and laterally to eliminate tilt, focus, and coma from the interference pattern. The axial position depends on the radius of curvature R, and like the autostigmatic test of primary mirrors, an error in R induces an error in the conic constant K of [19]

$$\frac{\Delta K}{K} = -\frac{\Delta R}{R}. \tag{9}$$

The secondary radius of curvature can be determine by measuring the gap between the test plate and the secondary, since the test plate radius and hologram functions are known.

4. FABRICATION OF HOLOGRAMS

The holograms are made using the rotational symmetry and writing one ring at a time using a special writing machine. The hologram writer uses a precise rotary stage to spin the test plate under a focused optical beam (See Fig. 12). Linear stages control the radial and axial position of the writing head. The axial motion is required to keep the beam focused on the curved surface. The pattern may be drawn by exposing photoresist, ablating a metallic coating, or by creating a thin oxidation layer by heating a metal coating with a focused laser. A prototype writer has been built at the Optical Sciences Center. The details of this instrument, and the results of its use for testing a 10.25-inch secondary mirror, are published in another paper in these proceedings.[1] The fabrication of zone plates by rotating the optic and writing one ring at a time has been performed by other groups on flat substrates to high accuracy.[11, 20] The holograms for testing secondary mirrors are in a unique domain where micron-scale errors are allowed, but the writer must work on large diameter, steeply curved surfaces. Line width is not important for the CGH test plate, so the writing process must only control the size of written features to 10%. Only the ring center position -- the center is defined to be halfway between the two edges -- must be held to a few microns. Hologram errors of 1 μm rms and 5 μm P-V degrade the surface measurement accuracy by only 3 nm rms and 20 nm P-V for the most difficult secondary mirror planned, the 120 cm LBT $f/4$.

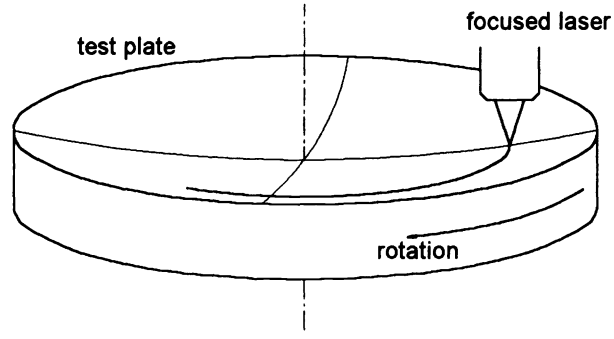

Figure 12. General geometry for optically writing ring patterns onto curved test plates. A focused laser beam is positioned radially and one ring at a time is exposed on the rotating optic.

The alignment of the hologram onto the test plate is not critical since this only affects the illumination which can tolerate milliradian-scale errors. It is important that the center of rotation is accurately found before writing the rings. An error in locating the center of rotation will cause a radial shift in the ring pattern which appears as a cone error in the diffracted wavefront.

5. RESULTS FROM PROTOTYPE TEST

A prototype test was performed to demonstrate the basic principles behind the measurement technique. An additional demonstration of the measurement of an aspheric secondary mirror is given in another paper in these proceedings.[1]

The first step in the development of this test was to perform a simple experiment to verify the concept of using a CGH test plate for metrology.[21] The test was simplified by using flat surfaces and linear rulings. The ruling pitch, illumination, imaging geometry, and measurement using phase shifting interferometry emulated the optical test of secondary mirrors. This test, shown in Fig. 13, verified that optical testing with a CGH test plate gives high contrast fringes that are insensitive to vibration and air currents. A 200-μm pitch ruling with distortion expected to be several microns was used to measure the surface figure of a small flat.

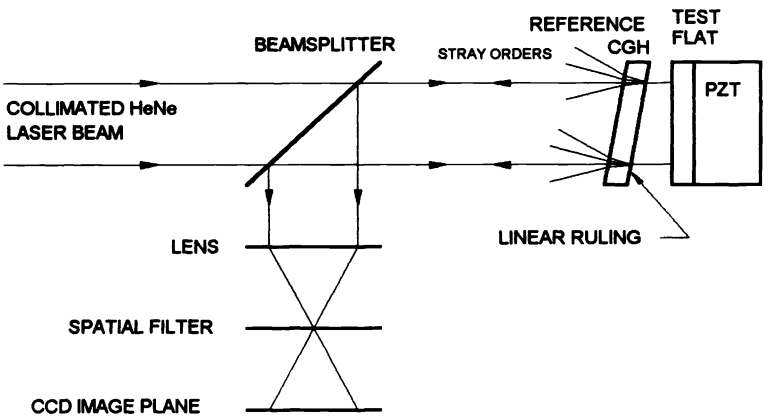

Figure 13. Optical layout of the setup used to verify the use of a CGH test plate.

The use of the CGH test plate was shown to have the high accuracy that was predicted. The fringes of interference had virtually perfect contrast and were easily phase shifted. There were some high frequency intensity variations caused by reflections from the window on the CCD and from laser speckle. These will be eliminated in the secondary mirror test by imaging onto a rotating ground glass disk and re-imaging onto the detector. Any other high frequency errors will be reduced by averaging several measurements and rotating the test plate.

The CGH was tilted to the appropriate angle to allow measurement of the test flat using the -1, 0, +1, and +5 diffracted orders. By using the fact that the CGH distortion causes errors proportional to the order number (Eq. 5), the surface figure and the grating writing errors were separated. As expected, the surface figure computed using all four maps is virtually identical to the measured zero order. A contour map of the test flat surface figure with respect to the reference surface is shown in Fig. 14. The measurement of the test flat with the first diffracted order from the CGH is shown in Fig. 15. This corresponds to the measurement of a secondary mirror with a CGH test plate. A direct subtraction between these two gives the error in the measurement, shown in Fig. 16.

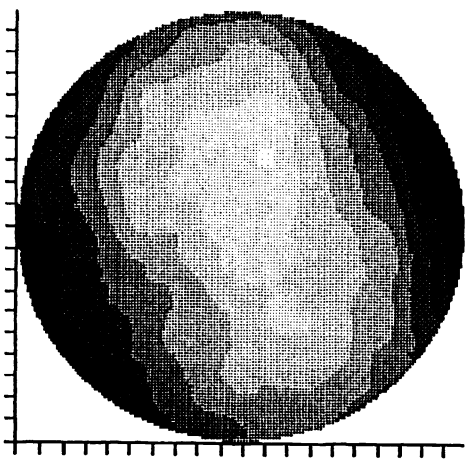

Fig. 14. Surface figure of test flat. The figure errors are 8.31 nm rms and 40.8 nm P-V. The contours shown are at 5 nm intervals.

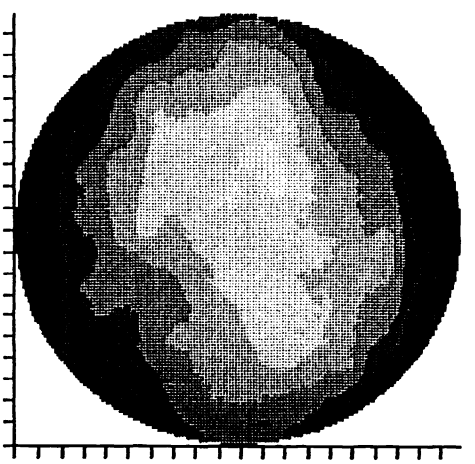

Fig. 15. Measured surface figure using the first diffracted order from the CGH. The figure errors are 7.60 nm rms and 38.3 nm P-V. The contours shown are at 5 nm intervals.

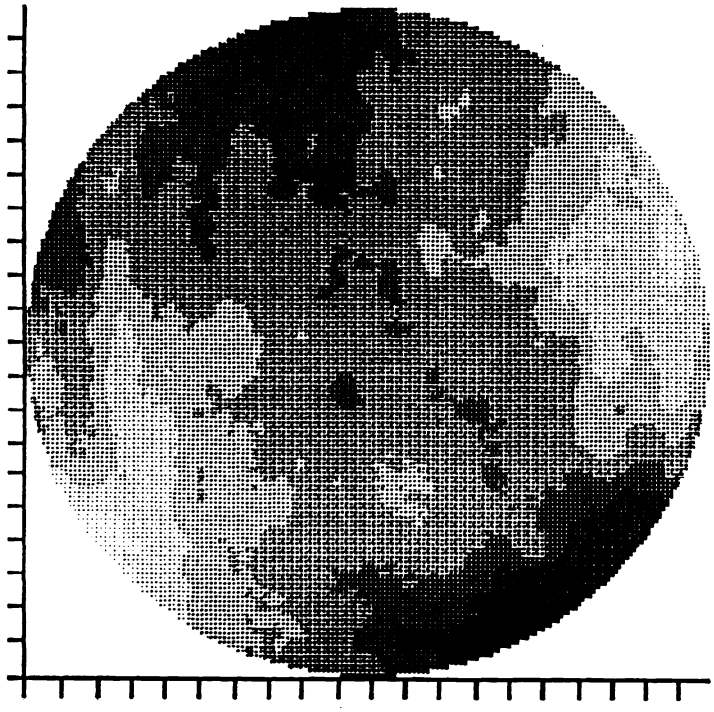

Fig. 16. Error in measuring test flat with CGH test plate. The figure errors are 2.09 nm rms and 13.6 nm P-V. The contours shown are at 2 nm intervals.

The measurement error shown in Fig. 16 has two components -- noise in the measurement and distortion in the CGH. These two effects were separated using the measurements at several orders. The noise in the measurement, caused mostly by the spurious fringes from the CCD window, was determined to cause 0.54 nm rms error. The ruling errors were determined to cause errors of 1.9 nm rms in the figure measurement. The spatial distortion in the 200 μm pitch ruling was determined to be 1.2 μm rms and 7.7 μm P-V with a spatial distribution shown by Fig. 16. This amount of distortion is consistent with the claims of the company that fabricated the rulings. It is also comparable to the writing accuracy expected in the fabrication of the test plates.

This test provided a quantitative demonstration that the principles behind the technique of interferometry using holographic test plates are valid.

6. TEST IMPLEMENTATION FOR LARGE SECONDARY MIRRORS

As mentioned above, the CGH test is planned for the convex aspheric secondary mirrors at the Steward Observatory Mirror Lab. Equipment for fabricating the holograms and for implementing the test is currently under construction. We plan to begin using the test in early 1995 to guide the stressed-lap polishing of the secondary mirror for the Sloan Digital Sky Survey Telescope.

6.1 LARGE HOLOGRAM WRITER

A second generation writing machine is being built that will write rings with an accuracy of 1 μm rms over surfaces with up to 180 cm diameter and with up to 100 mm surface sagitta. This machine uses a precise rotary air bearing driven at 4 rpm. The writing head is moved radially to 0.1 μm precision. The writing head position and tilt are measured interferometrically to 0.1 μm accuracy. The axial motion is controlled using a linear stage to keep the beam focused onto the test plate. The writing head uses an acousto-optic modulator to control the writing intensity and to scan the beam rapidly on the test plate. This rapidly moving spot creates an effective line focus that allows 100 μm wide lines to be written with a 4 μm focused spot.

6.2 ILLUMINATION SYSTEM

The test of the secondary mirrors will be performed with the optical surfaces *face down*, as they will be used in the telescopes. The test will be illuminated using a large aluminum shell aspheric reflector, as shown in Fig. 17. The aspheric reflector is made by polishing a sphere into the aluminum shell and bending in the asphericity. The edge will be constrained and sealed, and air pressure used to bend in the asphere. This will give a smooth, inexpensive aspheric surface. The low order errors such as astigmatism and spherical aberration have small slopes, so they do not strongly affect the test. We will use a 1.8-m reflector for most of the secondary mirror tests, and a second, more aspheric 2.5-m reflector for measuring the very large secondaries.

A small spherical convex reflector will relay the focus to the spatial filter and imaging system. Each secondary test requires a CGH test plate and illumination secondary. By putting the asphere on the large primary rather than the small illumination secondary, the imaging distortion is kept small.

The test plates, which are cast of borosilicate glass, are edge-supported using passive hydraulic actuators. Since the test plate reference surface is critical to the secondary test, it will be measured *in situ* by an interferometer from the center of curvature (using the 0-order diffraction from the hologram). Also, large azimuth bearings will allow the test plate to be rotated about the optical axis to determine the non-axisymmetric measurement errors. The test plate will be pushed with PZT's to allow high-resolution phase shifting interferometry.

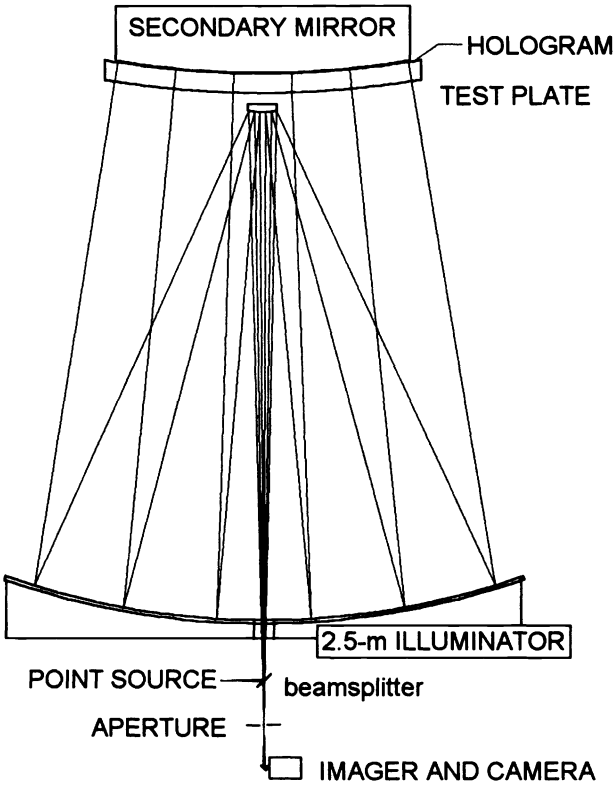

Figure 17. Illumination of CGH test for the MMT 1.7-m *f*/5 secondary mirror.

6.3 IMPLEMENTATION AT SOML

This test will become part of an integral facility being built at the Steward Observatory Mirror Lab. This facility, being constructed in the current polishing shop, is designed for rapidly fabricating the strongly aspheric secondary mirrors to high accuracy.[22] We will polish and grind the surfaces using the stressed-lap polishing technique[23,24] developed at the University of Arizona. Aspherizing and loose abrasive grinding with the stressed lap will be monitored using a swing arm profiler[25] that is mounted on the polishing machine. The CGH test will be performed on a tower adjacent to the 1.8-m stressed lap polishing machine. A transfer mechanism will efficiently move the optics from the test station shown in Fig. 17 to the polisher. The secondary test tower will allow *in situ* measurements of the spherical reference surface. This tower will also be used for measuring the concave secondaries planned for several telescope projects.

7. CONCLUSION

We have developed a new optical test for convex aspheres that appears to be optimal for measuring fast secondary mirrors. The accuracy of this test is achieved by using a reference spherical surface and a computer-generated hologram, both of which can be made and verified to high accuracy. Since the test is not affected by vibration and seeing, high-quality measurements can be quickly made. We are planning to use interferometric measurements with holographic test plates to provide accurate, efficient feedback to guide the fabrication of secondary mirrors at the Steward Observatory Mirror Lab.

REFERENCES

1 J. H. Burge, D. S. Anderson, T. D. Milster, and C. L. Vernold, "Measurement of a convex secondary mirror using a holographic test plate," in *Advanced Technology Optical Telescopes V*, L. M. Stepp, Editor, Proc. SPIE **2199**, (1994).

2 J. S. Loomis, "Computer-generated holography and optical testing," in *Recent Advances in Holography*, T. C. Lee and P. N. Tamura, Eds., Proc. SPIE **215**, 59-69 (1980).

3 K. Creath. and J. C. Wyant, "Holographic and speckle tests," in *Optical Shop Testing*, D. Malacara, Ed. (Wiley, New York, 1992) pp. 599-651.

4 E. N. Lieth and J. Upatnieks, "Reconstructed wavefronts and communication theory," J. Opt. Soc. Amer. **52**, 1123-1130 (1962).

5 B. R. Brown. and A. W. Lohmann, "Complex spatial filtering with binary masks," Appl. Opt. **5**, 967-969 (1966).

6 O. Bryngdahl and F. Wyrowski, "Digital holography -- computer-generated holograms," in *Progress in Optics* **28**, E. Wolf, ed. (Elsevier, New York, 1990) pp. 1-86.

7 J. C. Wyant. and V. P. Bennett, "Using computer-generated holograms to test aspheric wavefronts," Appl. Opt. **11**, 2833-2839 (1972).

8 S. M. Arnold, "How to test an asphere with a computer-generated hologram," in *Holographic Optics: Optically and Computer Generated*, I. N. Cindrich and S. H. Lee, Eds., Proc. SPIE **1052**, 191-197 (1989).

9 T. Yatagai and H. Saito, "Interferometric testing with computer-generated holograms: aberration balancing method and error analysis," Appl. Opt. **17**, 558-565 (1978).

10 A. F. Fercher, "Computer-generated holograms for testing optical elements: Error analysis and error compensation," Opt. Acta **23**, 347-365 (1976).

11 G. N. Buynov, *et al.*, "Holographic interferometric inspection of aspherical surfaces," *Optical Technology* **38**, 194-197 (1971).

12 Y. Ichioka and A. W. Lohmann, "Interferometric testing of large optical components with circular holograms," Appl. Opt. **11**, 2597-2602 (1972).

13 R. Mercier, "Holographic testing of aspheric surfaces," in *First European Conference on Optics Applied to Metrology*, M. Grosmann and P. Meyrueis, Eds., Proc SPIE **136**, 208-214 (1977).

14 R. Mercier and S. Lowenthal, "Comparison of in-line carrier frequency holograms in aspheric testing," Opt. Comm. **33**, 251-256 (1980).

15 J. H. Burge, "Certification of null correctors for primary mirrors," in *Advanced Optical Manufacturing and Testing IV*, J. Doherty, Editor, Proc. SPIE **1994**, 248-259 (1993).

16 J. W. Goodman, *Introduction to Fourier Optics*, (McGraw-Hill, San Francisco, 1968).

17 M. G. Moharam and T. K. Gaylord, "Rigorous coupled-wave analysis of metalic surface-relief gratings," JOSA A **3**, 1780-1787 (1986).

18 D. A. Gremaux and N. C. Gallagher, "Limits of scalar diffration theory for conducting gratings," Appl. Opt. **32**, 1948-1953 (1993).

19 J. H. Burge, *Advanced Techniques for Measuring Primary Mirrors for Astronomical Telescopes*, Ph. D. Dissertation, Optical Sciences, University of Arizona (1993).

20 V. P. Koronkevich, V. P. Kiriyanov, *et al.*, "Fabrication of kinoform optical elements," Optik **67**, No. 3, 257-266 (1984).

21 J. H. Burge and D. S. Anderson, "A full-aperture optical test for large convex aspheric mirrors," *Proc. Amer. Soc. for Precision Engineering* **8**, 29-32 (1993).

22 D. Anderson, H. Martin, J. Burge, D. Ketelsen, and S. West, "Rapid fabrication strategies for primary and secondary mirrors at Steward Observatory Mirror Lab," in *Advanced Technology Optical Telescopes V*, L. M. Stepp, Editor, Proc. SPIE **2199**, (1994).

23 S. C. West, *et al.*, "Practical design and performance of the stressed lap polishing tool," submitted to Appl. Opt. (1994).

24 H. M. Martin, *et al.*, "Progress in the stressed-lap polishing of an 1.8-m *f*/1 mirror," in *Advanced Technology Telescopes IV*, L. D. Barr, Editor, Proc. SPIE **1236**, 682-690 (1990).

25 D. S. Anderson and R. E. Parks, "Versatile profilometer for aspheric optics," in *Technical Digest on Optical Fabrication and Testing, 1990* (Optical Society of America, Washington D.C., 1990) pp. 119-122.